X-Ray Backlit Imaging of Indirect-Drive Capsule Implosions

D. H. Kalantar
C. J. Keane
S. W. Haan
O. L. Landen
B. A. Hammel
D. H. Munro

Introduction

In indirectly driven inertial confinement fusion (ICF),[1] a fusion capsule is bathed in broadband soft x rays created inside a hohlraum. The x-ray drive ablates material from the outer capsule surface, causing the inner wall (pusher) of the capsule to implode and compress the fuel. Both the efficiency of the implosion and the growth of hydrodynamic instabilities at the ablation surface (Rayleigh-Taylor instability)[2] vary with the aspect ratio of the imploding capsule.[3–5]

Capsules illuminated by a broadband soft x-ray drive experience preheat due to the harder component of x rays. To maintain a low adiabat for the fuel and pusher during the implosion, it is necessary to shield them from the harder x rays. This is done by introducing dopants in the capsule ablator material. The dopant added to the ablator prevents the harder x rays from preheating the pusher and, as a result, maintains a higher density as well as a sharper density gradient in the pusher increasing both the implosion efficiency and hydrodynamic instability growth. The doped ablator also has a higher initial aspect ratio because it has a higher initial density and a lower mass ablation rate.

We use x-ray backlighting to measure the in-flight areal density of the pusher in both Ge-doped and undoped x-ray driven imploding capsules. Previous images of an indirectly driven implosion provided a measure of the implosion velocity and low-mode distortion.[6] We recorded large-area backlit images, performed radial intensity lineouts, and unfolded a radial density profile. Postprocessed simulations are in good agreement with the measurements.

X-Ray Backlighting on Nova

We used x-ray backlighting techniques[7] to image an x-ray driven implosion capsule on the Nova laser.[8] The plastic capsules consisted of a 3-μm-thick polystyrene shell, a 3-μm-thick layer of polyvinyl alcohol (PVA), and an ablator layer coated on the outside. The polystyrene ablators were 34 μm thick with 2.5% Ge by atomic fraction, or 50 μm thick with no dopant to match the implosion velocities. The outside diameter of the capsules was about 510 to 530 μm. The capsules were filled to 50 atm pressure with an equal mixture of hydrogen and deuterium.

The backlighter target is shown in Figure 1. The ICF capsule was placed at the center of a cylindrical gold hohlraum that was 1.6 mm in diameter and 2.5 mm long. There were two 650-μm-diam diagnostic access holes in the hohlraum, positioned on opposite sides at the midplane of the hohlraum. These were covered with 150-μm-thick CH foils to fill the hohlraum with a low-mass plasma and restrict the flow of emissive gold plasma into the diagnostic line of sight. A thin foil used for backlighting was positioned approximately 3 mm from the center of the hohlraum, collinear with the capsule diagnostic holes and diagnostic line of sight.

We used eight Nova beams at 0.35 μm to create an x-ray drive in the hohlraum. The beams were pointed inside the hohlraum through the laser entrance holes so that they were distributed symmetrically around the azimuth of the hohlraum with a fourfold rotation symmetry. The 2.2-ns shaped laser pulse had an intensity contrast from the foot to the peak of 1:6 (Figure 2). A total of 25 kJ of laser energy was delivered into the hohlraum, with a peak laser power of 19 TW. The x-ray drive temperature in the hohlraum is shown in Figure 2. It peaks at about 200 eV at 1.8–2.0 ns.

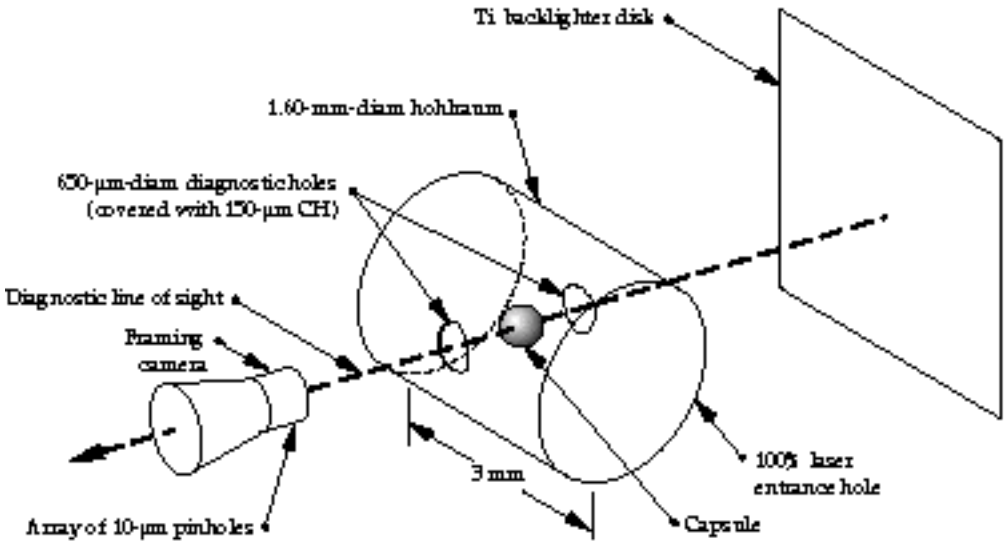

FIGURE 1. Diagram of the backlighter target used on Nova. (20-03-0397-0446pb01)

Two frequency-doubled Nova beams were focused onto the backlighter foil. These were configured with random phase plates and focused to an ~700-μm focal spot on the backlighter foil at about 5×10^{14} W/cm^2 to generate a large-area source of backlighter x rays. The laser pulse shape on these two beams was 2 ns square, which gave us a constant intensity of x rays.

For imaging the Ge-doped capsules, we used a Ti backlighter foil and recorded the images filtered with a 12-μm Ti filter. This provided a nearly monochromatic image, principally in 4.7 keV emission from the 1s2p–1s^2 line of Ti (Figure 3). For the undoped implosion capsules, we used a Rh backlighter and filtered the images with a 12-μm Sc filter. This provided a narrow-band spectrum at about 3–3.5 keV.

We recorded the radiograph images of the fusion capsule at various times during the implosion using a gated x-ray framing camera.[9,10] The timing of the backlighter beams was varied in order to record images over approximately 3 ns. The camera had a full width at half maximum gate width of 55 ps. We used an array of 10-μm pinholes at 8× magnification, overlaid with a 250-μm-thick collimator that had 50-μm-diam holes to limit the hard x-ray background in each pinhole image.

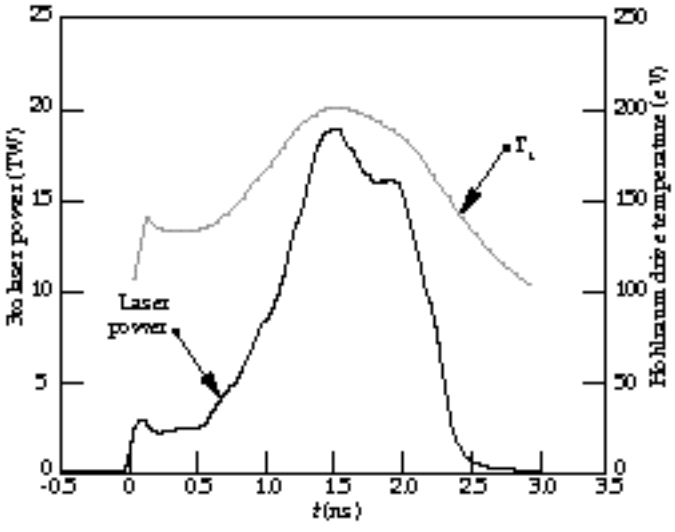

FIGURE 2. Laser power and hohlraum x-ray drive temperature as a function of time. (20-03-0397-0447pb01)

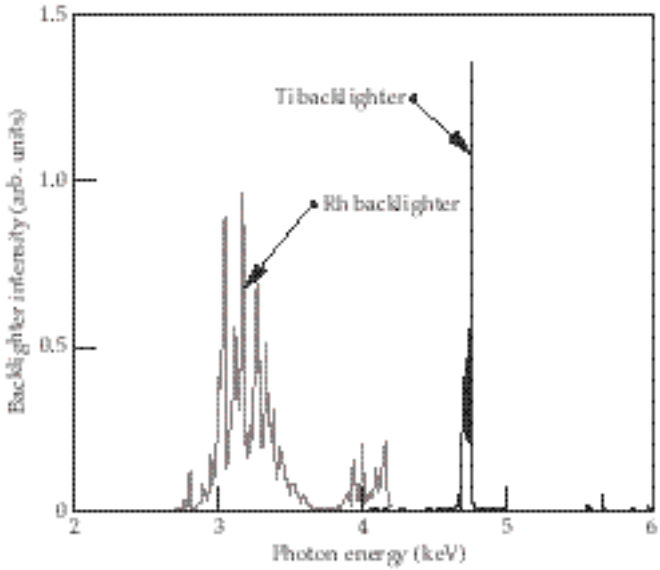

FIGURE 3. Ti and Rh x-ray backlighter spectra. (20-03-0397-0448pb01)

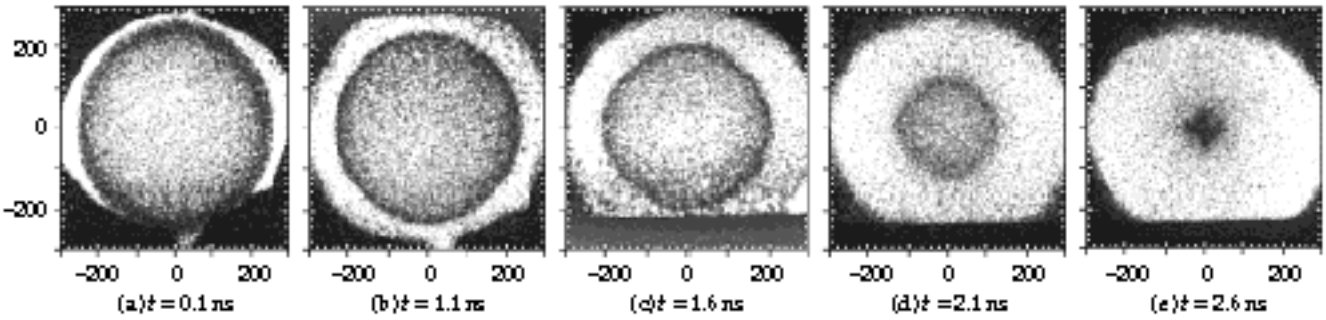

FIGURE 4. Series of x-ray backlit images of a Ge-doped capsule recorded at t = 0.1, 1.1, 1.6, 2.1, and 2.6 ns. The scales are in microns at the target. (20-03-0397-0449pb01)

Backlit Images of a Ge-Doped Implosion Capsule

Figure 4 shows a series of backlit images from Ge-doped capsules. These images are shown corrected for the diagnostic flat-field and for the spatial intensity profile of the x-ray backlighter. These images were obtained on two Nova target shots. For each shot, the capsule had an initial outer radius of 255 μm.

We imaged the backlighter foil from the rear side using a second x-ray framing camera. The Ti backlighter foil was 12 μm thick, so that these images of the foil were filtered identically to the backlit images of the implosion capsule. The flat-field characterization incorporating the gain degradation in each strip line for both framing cameras and the overall backlighter intensity profile were applied to normalize the backlit images.

We tested that the backlit implosion images of Ge-doped capsules were nearly monochromatic by measuring the initial contrast of the undriven capsule shell in the backlighter x rays. We compared the fractional transmission of backlighter x rays through the center of the capsule with the unattenuated backlighter intensity. Based on the composition of the Ge-doped capsule shell, the calculated transmission through twice the total wall thickness is about 0.47. For the image shown above in Figure 4a, we measured a fractional transmitted intensity of 0.45 in the center of the image.

In-Flight Pusher Density Profile

We calculated radial density profiles by performing an Abel inversion of the radial lineouts for each image. Since the late-time images shown in Figure 4 have a P4 asymmetry, the radial lineouts were averaged over 45° segments in the polar direction, as indicated schematically in Figure 5. Up to eight individual lineouts per image were Abel inverted by assuming azimuthal symmetry for each.

Abel-inverted lineouts from Ge-doped capsules are shown at five different times in Figure 6. These are

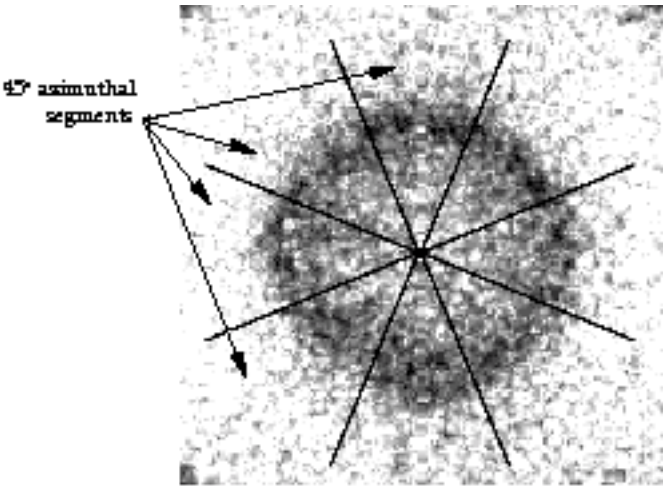

FIGURE 5. Schematic showing the wedge segments that were averaged in the polar direction to perform the radial lineouts of the backlit images. (20-03-0397-0450pb01)

plotted as the product of opacity times density. Since the shock-preheated ablator is at a temperature of <<100 eV, the opacity of the Ge-doped ablator material at the backlighter energy of 4.7 keV (dominated by L-shell Ge and K-shell carbon) is nearly identical to the cold material opacity. Therefore, these lineouts are proportional to the density profile of the capsule pusher. Note that we have smoothed the inverted lineouts at small radius. The polar average smooths the radial lineout at large radii, but noise statistics and speckle of the microchannel plate detector and backlighter profile dominate at small radii.

We used LASNEX[11] to model the implosion of the Ge-doped capsule. The conditions of the pusher in the Ge-doped capsule implosions were calculated, and the output was postprocessed to generate simulated images with the backlighter spectrum shown in Figure 3, at the same times of the images shown in Figure 4. These images were then convolved with the instrument resolution expected of a 10-μm pinhole

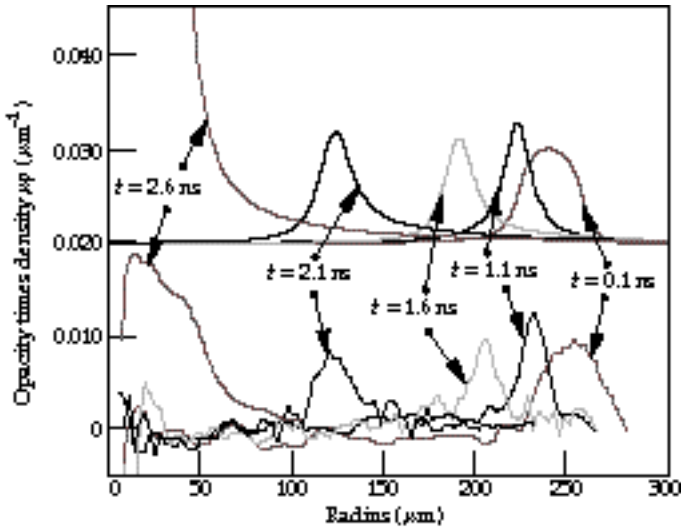

FIGURE 6. Radial density profiles calculated by Abel-inverting radial lineouts of the x-ray transmission through the capsule (bottom curves). Results from postprocessed simulated images are shown for comparison (top curves). (20-03-0397-0451pb01)

and unfolded by Abel inversion using the same assumptions about spherical symmetry and monochromatic imaging. The resulting Abel-inverted simulated lineouts are shown overlaid in Figure 6. These show a time history similar to the experimental lineouts.

We measured the radius of the half-maximum density on the outer edge of the Abel-inverted lineouts. This is shown in Figure 7, plotted with the aspect ratio that we calculate as the ratio of the average radius to the full width at half maximum of the radial density profile for each time. Note that the error bars represent the standard error in the mean, based on an average from the 45° lineouts.

The radius and aspect ratio calculated from the postprocessed simulated images are shown in Figure 7 as solid curves. These values were calculated from the Abel-inverted lineouts of the simulated images in the same manner as the values measured in the experiment. The simulations are in good agreement with the measurement.

Undoped Implosion Capsules

X-ray backlit images of undoped capsules were obtained throughout the implosion with a Rh backlighter. We performed radial lineouts over the same 45° segments to obtain radial density profiles at each time. The average radius and aspect ratio, measured as described above, are shown as a function of time in Figure 8.

The results from postprocessed simulated images are shown overlaid in this figure by the solid curves. Note that the undoped capsules are expected to decompress more due to less preheat shielding, which lowers their late-time ($t > 1.5$ ns) aspect ratio, as measured by comparing Figures 7 and 8. The fact that the aspect ratio is lower for the undoped capsules than for the doped capsules early in time is because it was necessary to use an initially thicker undoped ablator to match the implosion velocities for the different cases.

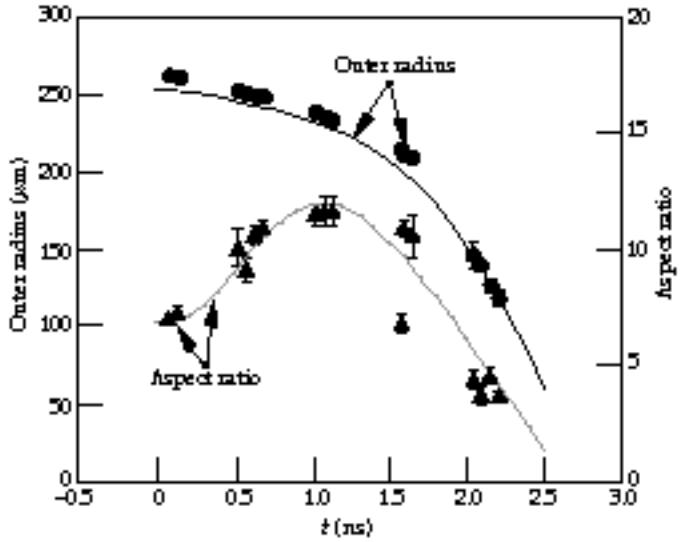

FIGURE 7. Radius and aspect ratio calculated from the Abel-inverted lineouts of Ge-doped backlit images as a function of time (data points). Results from postprocessed simulated images are shown for comparison (curves). (20-03-0397-0452pb01)

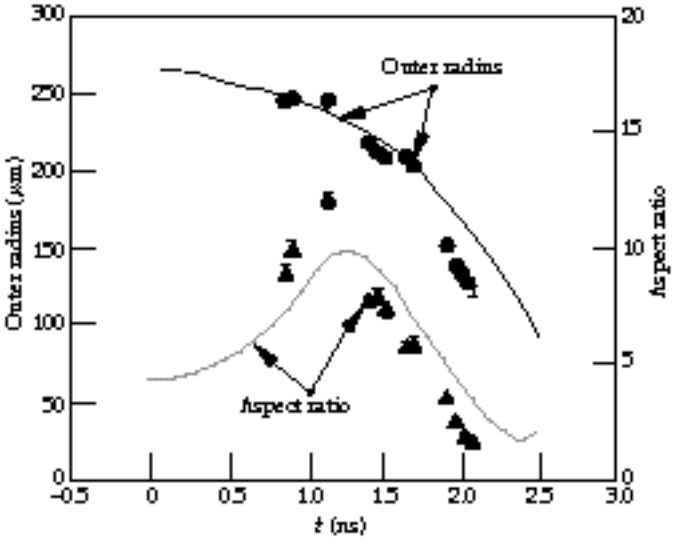

FIGURE 8. Radius and aspect ratio calculated from the Abel-inverted lineouts of undoped backlit images as a function of time (data points). Results from postprocessed simulated images are shown for comparison (curves). (20-03-0397-0453pb01)

Summary

We have used x-ray backlighting techniques to record images of indirectly driven ICF capsules on Nova. These large-area images provide quantitative information about the in-flight pusher density profile as a function of time. We measure the in-flight aspect ratio of imploding Ge-doped and undoped capsules using an 8-beam pulse-shape–26 drive. The doped results and simulations match well. The results from the undoped capsules do not agree as well. These results should be more sensitive to preheat levels, which would otherwise be difficult to measure. Detailed comparisons with modeling in which the preheat level is varied in the simulations will allow a better characterization of the preheat levels.

Acknowledgments

We acknowledge the support of the diagnostic development group at Nova and the collaboration with D. Bradley of the Laboratory for Laser Energetics at the University of Rochester in developing the fast framing camera we used for these experiments.

Notes and References

1. J. Lindl, *Phys.Plasmas* **2**, 3933 (1995).
2. Lord Rayleigh, *Scientific Papers,* Vol. II, p. 200, Cambridge Univ. Press (1900).
3. O. L. Landen, C. J. Keane, B. A. Hammel, W. K. Lovedahl, et al., "Effects of variable x-ray preheat shielding in indirectly-driven implosions," to appear in *Phys. Plasmas* **3**, 2094 (1996).
4. O. L. Landen, C. J. Keane, B. A. Hammel, M. D. Cable, et al., *J. Quant. Spectrosc. Radiat. Transfer* **54**, 245 (1995).
5. C. Keane, G. W. Pollak, R. C. Cook, T. R. Dittrich, et al., *J. Quant. Spectrosc. Radiat. Transfer* **54**, 207 (1995).
6. M. Katayama, H. Shiraga, M. Nakai, T. Kobayashi, and Y. Kato, *Rev. Sci. Instrum.* **64**, 706 (1993).
7. S. G. Glendinning, P. Amendt, K. S. Budil, B. A. Hammel, et al., *Applications of Laser Plasma Radiation II*, edited by M. C. Richardson and G. A. Kyrala, in *Proc. SPIE* (Society of Photo-optical Instrumentation Engineers, Bellingham, WA, 1995), vol. 2523, pp. 29–39.
8. E. M. Campbell, J. T. Hunt, E. S. Bliss, D. R. Speck, and R. P. Drake, *Rev. Sci. Instrum.* **57**, 2101 (1986).
9. D. K. Bradley, P. M. Bell, O. L. Landen, J. D. Kilkenny, and J. Oertel, *Rev. Sci. Instrum.* **66**, 716 (1995).
10. P. M. Bell, J. D. Kilkenny, O. L. Landen, D. K. Bradley, et al., *Ultrahigh and High Speed Photography, Videography, and Photonics '94*, in *Proc. SPIE* (Society of Photo-optical Instrumentation Engineers, Bellingham, WA, 1994), p. 234.
11. G. B. Zimmerman and W. L. Kruer, *Comments Plasma Phys. Controlled Fusion* **2**, 51 (1975).